Atmos. Meas. Tech., 7, 1957–1968, 2014
www.atmos-meas-tech.net/7/1957/2014/
doi:10.5194/amt-7-1957-2014

Atmospheric Measurement Techniques
Open Access

Airborne emission measurements of SO_2 , NO_x and particles from individual ships using a sniffer technique

J. Beecken[1], J. Mellqvist[1], K. Salo[1], J. Ekholm[1], and J.-P. Jalkanen[2]

[1]Chalmers University of Technology, Earth and Space Sciences, Gothenburg, Sweden
[2]Finnish Meteorological Institute, Helsinki, Finland

Correspondence to: J. Beecken (beecken@chalmers.se)

Received: 12 July 2013 – Published in Atmos. Meas. Tech. Discuss.: 9 December 2013
Revised: 9 May 2014 – Accepted: 27 May 2014 – Published: 3 July 2014

Abstract. A dedicated system for airborne ship emission measurements of SO_2, NO_x and particles has been developed and used from several small aircraft. The system has been adapted for fast response measurements at 1 Hz, and the use of several of the instruments is unique. The uncertainty of the given data is about 20 % for SO_2 and 24 % for NO_x emission factors. The mean values with one standard deviation for multiple measurements of 158 ships measured from the air on the Baltic and North Sea during 2011 and 2012 show emission factors of $18.8 \pm 6.5\,g\,kg_{fuel}^{-1}$, $66.6 \pm 23.4\,g\,kg_{fuel}^{-1}$ and $1.8 \pm 1.3\,10^{16}$ particles kg_{fuel}^{-1} for SO_2, NO_x and particle number, respectively. The particle size distributions were measured for particle diameters between 15 and 560 nm. The mean sizes of the particles are between 45 and 54 nm dependent on the distance to the source, and the number size distribution is monomodal. Concerning the sulfur fuel content, around 85 % of the monitored ships comply with the International Maritime Organization (IMO) limits. The reduction of the sulfur emission control area (SECA) limit from 1.5 to 1 % in 2010 appears to have contributed to reduction of sulfur emissions that were measured in earlier studies from 2007 to 2009. The presented method can be implemented for regular ship compliance monitoring.

1 Introduction

Ships emit large quantities of air pollutants, and it is necessary to reduce these to improve air quality (Corbett et al., 2007; European Commission, 2009). Most countries have ratified the International Maritime Organization (IMO) Marpol Annex VI protocol, and the EU has adopted directive 2012/33/EU, which sets limits on nitrogen oxides (NO_x) and sulfur dioxide (SO_2) emissions from ship exhausts. The regulation includes a global cap of sulfur fuel content (SFC) and contains provisions allowing for establishment of special SO_2 and NO_x emission control areas (ECAs), i.e., SECA (for sulfur) and NECA (for nitrogen oxide). The Baltic Sea, the North Sea, English Channel and the coastal waters around the US and Canada are designated as SECA, with the North American area as a NECA. Following the IMO regulation there will be a global cap for the allowed maximum content of sulfur in fuel of 0.5 % from the year 2020. In the SECAs the used SFC must not exceed 0.1 % beginning in 2015. The IMO regulation regarding NO_x is more complicated than for SO_2, since NO_x production is dependent on the nature of the combustion process rather than being related to fuel composition. IMO has therefore chosen emission limits (resolution MEPC.177(58)) that correspond to the total NO_x emission in grams per axial shaft energy produced from the engine in kWh. These limits depend on the engine type and are therefore given versus the rated rotational speed of the specific engines. Ships built between 2000 and 2010 should emit less than a certain limit (Tier 1), while ships built after 2011 should emit 20 % less (Tier 2). In NECA the emissions should be 80 % lower than Tier 1 by 2016 (Tier 3), although this time limit is presently being renegotiated within IMO.

There are several ways available for the shipping companies to adapt to the new regulations. It is possible to use alternative fuel, i.e., liquefied natural gas (LNG) or methanol. Abatement techniques to reduce both NO_x and SO_2 emissions are available. However these possibilities are often limited due to high costs for investments in technologies which are under ongoing development. Therefore it is believed that there will be a higher demand for and higher prices on low-sulfur fuels in the future.

In the SECA the cost for ship transport will increase by 50–70 % due to increased fuel costs (Kalli et al., 2009). There will hence be considerable economic incentive not to comply with SECA regulations. Today the fuel of the ships is controlled by port state control authorities conducting random checks of bunker delivery notes, fuel logs and occasional fuel sample analyses in harbors. This is time consuming and few ships are being controlled. There is no available technique able to control what fuel is used on the open sea, and in general it is considered easy to tamper with the usage of fuel, especially since ships use several tanks, often with different fuels.

Here we present airborne emission measurements of emission factors in mass of emitted pollutant per amount of consumed fuel for individual ships. One valuable use of such data is as input data for modeling of the environmental impact of shipping. A new type of ship emission model that has emerged recently calculates instantaneous emissions of ships based on ship movement from Automatic Identification System (AIS), ship propulsion (Alföldy et al., 2013) calculations and emission factors (Jalkanen et al., 2009, 2012). The latter are taken from laboratory tests and occasional onboard measurements (Moldanova et al., 2009; Petzold et al., 2004, 2008). The emission factors depend on engine type, fuel type, use of abatement equipment and load. In general there are large uncertainties in the emission factors for some species, such as particles, and within the SECAs there is additional uncertainty as to how well the IMO legislation will be respected regarding fuel use and abatement technologies. There is hence substantial need for efficient techniques for remote measurements of real ship emissions.

The airborne sniffer system described here has been developed as part of a Swedish national project named Identification of Gross Polluting Ships (IGPS) (Mellqvist et al., 2008; Mellqvist and Berg, 2014, 2010) aimed at developing a remote surveillance system to control whether individual ships obey the IMO legislation of reduced SFC and NO_x emissions, as discussed above (Alföldy et al., 2013). The sniffer system is usually combined with an optical system (Mellqvist and Berg, 2014) that can be used as a first alert system and also to quantify the emission in grams per second, but this will not be discussed further here.

The principle of the sniffer method is to obtain emission factors in grams pollutant per kilogram fuel by measuring the ratio of the concentration of the pollutant versus the concentration of CO_2, inside the emission plume of the ships. This principle has been employed in several other studies from the air, ships and harbors (Sinha et al., 2003; Chen et al., 2005; Mellqvist et al., 2008; Alföldy et al., 2013; Balzani Lööv et al., 2013; Mellqvist and Berg, 2014), though in most cases for a relatively small number of vessels. Here we demonstrate a dedicated system meant for routine surveillance of ship emissions from small airplanes and other platforms. The system includes a fast electrical mobility system to measure particle number size distribution, used here in flight for the first time and a custom-made cavity ring-down system for fast airborne plume measurements of CO_2 and CH_4. In addition we show unique measurements from 158 individual ships carried out on several occasions per ship in the North and Baltic Sea from a helicopter and two different airplanes during 2011 and 2012. These data are compared to data from 2007/2008 (Mellqvist and Berg, 2010, 2014). The emission data for the individual ships have been interpreted against IMO limits and ship and engine type. This paper gives recommendations for how future compliance monitoring of ship emissions could be carried out.

2 Methods

In this section the instrumentation, calibration methods and uncertainties are presented. A description of the measurement campaigns and the plume sampling procedure is given here.

2.1 Instrumentation

With the setup presented herein concentrations of CO_2, SO_2, NO_x and submicron aerosol particles are measured.

2.1.1 CO_2 instrumentation

A flight-modified Picarro G2301-m is used to monitor the concentration of CO_2 in the air. This instrument is a greenhouse gas monitor based on cavity ring-down spectroscopy (CRDS) (O'Keefe and Deacon, 1988) which was specially modified for use in aircraft. The instrument is capable of measuring CO_2, CH_4 and relative humidity (RH), the latter for correction issues. The measurements are conducted sequentially with a time response t_{90}, i.e., the time to reach from 10 to 90 % of the sample value of less than 1 s. The measurement mode was modified in order to obtain as many measurements as possible during the short time in which the aircraft traverses a plume. Depending on the needs, a low- or high-flow mode can be selected, with either one or two CO_2 measurements per second for each flow setting. In the latter case, the time slot for the measurement of CH_4 is replaced by a second CO_2 sample within the same sequence. During the conducted measurement flights the high-flow, 2 Hz CO_2 mode was used.

2.1.2 SO_2 instrumentation

A modified Thermo 43i-TLE trace gas monitor was applied. This instrument analyzes the volume mixing ratio of SO_2, VMR(SO_2), in air by stimulating fluorescence by UV light (Luke, 1997). The detected intensity of fluorescence light is proportional to the volume mixing ratio of SO_2 molecules in the sample gas. In order to gain a higher flow for faster sampling, a hydrocarbon stripper and the flow meter were removed from the monitor, which resulted in

a flow rate of 6 LPM. The t_{90} is about 2 s and the sample rate was set to 1 Hz. The Thermo 43i-TLE shows some cross-response to NO and polycyclic aromatic hydrocarbons (PAH). The VMR(SO_2) reading increases by 1.5 % of the actual VMR(NO). In this study, this error was reduced by simultaneous measurements of NO_x assuming that the fraction of NO is 80 % (Alföldy et al., 2013). The corrected SFC value was on average 6 % ± 8 % below the uncorrected, NO-interfered SFC value. The cross-response of PAH is not important since these species are only present at small levels in ship plumes (Williams et al., 2009).

2.1.3 NO_x instrumentation

The NO_x measurements were performed with a Thermo 42i-TL trace gas monitor. This instrument measures the VMR(NO) by chemiluminescence caused by the reaction of NO with ozone (Kley and McFarland, 1980). The intensity of the detected chemiluminescent light is proportional to the VMR(NO) molecules. In order to measure the volume mixing ratio of NO_x, the instrument was run in a mode in which NO_2 is first converted to NO. The sample flow was 1 LPM, which results in t_{90} of less than 1 s and the sample rate 1 Hz.

2.1.4 Particle instrumentation

The particle number size distributions ranging from 5.6 to 560 nm of the emitted plumes were also measured in flight. This was done using the TSI 3090 engine exhaust particle sizer (EEPS). The EEPS is developed for monitoring of size distributions of aerosol particles in exhaust gases from combustion engines. It features 10 Hz simultaneous sampling of 32 measurement channels between 5.6 and 560 nm and has a sample flow of 10 LPM with a t_{90} of 0.5 s. The data were integrated for 1 s intervals. Particles in the sample air are charged and size selected according to the size-dependent mobility in an electrical field (Johnson et al., 2004). The charged particles' impact on electrometer plates and the number concentrations in the different size bins are achieved as the generated current. The EEPS has been used for onboard monitoring of ship emissions (Hallquist et al., 2013) and stationary ship plume measurements (Jonsson et al., 2011) in earlier studies. The EEPS was found to be suitable for this kind of airborne plume measurements and was to our knowledge used here for the first time on an aircraft. When the EEPS was operated onboard an airplane, it was connected to an isokinetic inlet for which the flow was optimized for the airspeed during plume measurement. There was no isokinetic inlet used for the helicopter-based measurements, because the airspeed of the helicopter during measurement was much lower.

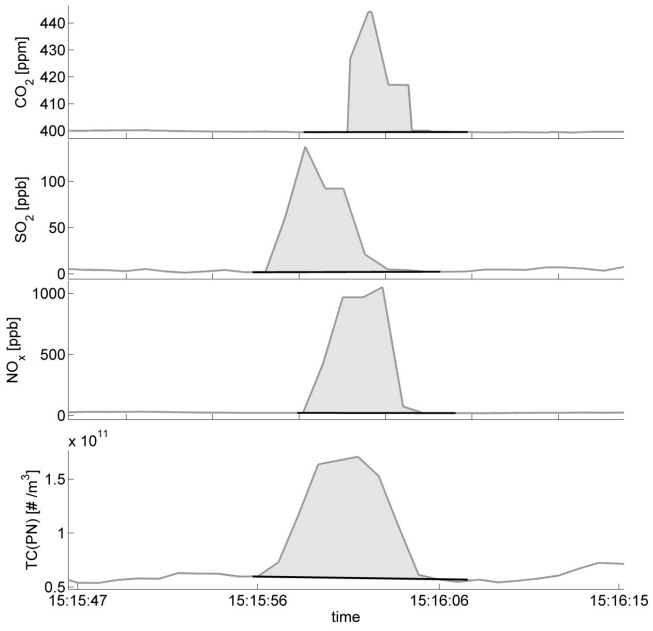

Figure 1. Example of a plume transect measurement. The volume mixing ratios of CO_2, SO_2 and NO_x are measured. The presented total concentration of particles, TC(PN), is calculated from the measurement of the particle number over size distribution. The volume mixing ratios and particle concentration above the respective baselines (black line) are summed up along the transect path. The ratio of the areas (light grey) for SO_2, NO_x and TC(PN) to CO_2 is proportional to the respective emission factor expressed in g kg_{fuel}^{-1} and particles kg_{fuel}^{-1}.

2.2 Calculation of emission factors

Emission factors in weight g kg_{fuel}^{-1} or particles kg_{fuel}^{-1} are obtained as the ratio of the pollutant x versus the volume mixing ratio of CO_2. In practice the volume mixing ratios of all measured species are first summed along the plume transect ($\sum[x]$), and then these values are normalized against the corresponding sum for CO_2. In Fig. 1 the volume mixing ratios for CO_2, SO_2 and NO_x and the total concentration of particle number are shown for one transect through the emission plume.

The carbon fuel content is required for the calculation of the emission factors. Studies show it is 87 ± 1.5 % for marine gas oil, marine diesel oil and residual oil (Cooper, 2003; Tuttle, 1995). For the calculations it is assumed that this fraction remains unchanged after fuel burning and that all burnt carbon is emitted as CO_2. Hence the SO_2 emission factor, EF(SO_2), in grams per kilogram fuel using the atomic and molar masses for C and SO_2, respectively, can be calculated by

$$\mathrm{EF}(\mathrm{SO_2})\left[\mathrm{g\,kg_{fuel}^{-1}}\right] = \frac{m(\mathrm{SO_2})}{m(\mathrm{fuel})}$$
$$= \frac{M(\mathrm{SO_2})\cdot\sum\left[\mathrm{SO_{2,ppb}}\right]}{M(C)/0.87\cdot\sum\left[\mathrm{CO_{2,ppm}}\right]} = 4.64\frac{\sum\left[\mathrm{SO_{2,ppb}}\right]}{\sum\left[\mathrm{CO_{2,ppm}}\right]}. \quad (1)$$

The values of SO_2 were corrected for the interference of NO. The cross-sensitivity of the modified instrument was experimentally found to be 1.5 %. A NO-to-NO_x molar ratio of around 80 % is assumed (Alföldy et al., 2013). Hence, for samples where NO_x was measured, $\sum[SO_2]$ was subtracted by 1.2 % of $\sum[NO_x]$ over the same plume sample. For samples without measured NO_x data, calculated data from the STEAM model (Jalkanen et al., 2009, 2012) for the NO_x-to-CO_2 ratios multiplied with measured CO_2 data were used for the correction instead. Where neither measured nor modeled NO_x data were available, the EF(NO_x) was assumed to be 65 $\mathrm{g\,kg_{fuel}^{-1}}$, which was the median value of the measured EF(NO_x) of other ships. The missing NO_x data for correction of the SO_2 data were then retrieved with Eq. (3) in combination with the measured CO_2 data. For the calculation of the SFC, it is assumed that all sulfur is emitted as SO_2. Hence the SFC is calculated by

$$\mathrm{SFC}[\%] = \frac{m(S)}{m(\mathrm{fuel})} = \frac{M(S)\cdot\sum\left[\mathrm{SO_{2,ppb}}\right]}{M(C)/0.87\cdot\sum\left[\mathrm{CO_{2,ppm}}\right]}$$
$$= 0.232\frac{\sum\left[\mathrm{SO_{2,ppb}}\right]}{\sum\left[\mathrm{CO_{2,ppm}}\right]}. \quad (2)$$

The NO_x emission factor in grams per kilogram fuel is calculated accordingly in Eq. (3). Most of the NO_x emission is in form of NO (Alföldy et al., 2013). Nonetheless, for these calculations the molecular mass of NO_x is assumed to be the molecular mass of NO_2 following IMO guidelines (MEPC, 2008).

$$\mathrm{EF}(\mathrm{NO_x})\left[\mathrm{g\,kg_{fuel}^{-1}}\right] = \frac{m(\mathrm{NO_x})}{m(\mathrm{fuel})} =$$
$$\frac{M(\mathrm{NO_2})\cdot\sum\left[\mathrm{NO_{x,ppb}}\right]}{M(C)/0.87\cdot\sum\left[\mathrm{CO_{2,ppm}}\right]} = 3.33\frac{\sum\left[\mathrm{NO_{x,ppb}}\right]}{\sum\left[\mathrm{CO_{2,ppm}}\right]} \quad (3)$$

The specific fuel oil consumption (SFOC) in terms of mass of consumed fuel per axial shaft power is retrieved from the STEAM model (Jalkanen et al., 2009, 2012). It corresponds to SFOC data supplied by the engine manufacturer through IHS Fairplay World Shipping Encyclopedia (IHS, 2009), corrected for the estimated load from the ship speed using correction curves supplied by engine manufacturers. The current SFOC value for the measured ship was taken from the STEAM model as a function of the ship's speed at the time of the measurement. The SFOC data are used for the calculation of the NO_x emission per produced energy $EF_{kWh}(NO_x)$ in

$$\mathrm{EF_{kWh}(NO_x)}\left[\mathrm{g\,kWh^{-1}}\right] = \mathrm{EF}(\mathrm{NO_x})\cdot\mathrm{SFOC(load)}. \quad (4)$$

The emission factor for particle number EF(PN) is calculated in Eq. (5) as the sum of the total concentration of the particle number, $\sum$[PN], with an assumed emission factor of CO_2 of 3.2 $\mathrm{kg\,kg_{fuel}^{-1}}$ (Hobbs et al., 2000).

$$\mathrm{EF(PN)}\left[\mathrm{particles\,kg_{fuel}^{-1}}\right] = \frac{\sum[\mathrm{PN}]}{\sum[\mathrm{CO_2}]}\cdot\mathrm{EF}(\mathrm{CO_2}) \quad (5)$$

It is known that the diesel particle density varies with composition and size (Barone et al., 2011; Virtanen et al., 2002). For the calculation of the particle mass distribution in this paper, the particle density is arbitrarily assumed to be 1 $\mathrm{g\,cm^{-3}}$. The emission factor for particle mass, EF(PM), is then calculated correspondingly to Eq. (5) by substituting $\sum$[PN] with $\sum$[PM].

The geometric mean diameter (GMD) and the corresponding geometric standard deviation (GSD) were calculated for the size-resolved particle number concentrations by

$$\mathrm{GMD}[\mathrm{nm}] = \exp\left(\frac{\sum\left[n\cdot\ln\left(D_\mathrm{p}\right)\right]}{N}\right) \quad (6)$$

and

$$\mathrm{GSD}[\mathrm{nm}] =$$
$$\exp\left(\left[\frac{\sum\left[n\cdot\left[\ln\left(D_\mathrm{p}\right)-\ln(\mathrm{GMD})\right]^2\right]}{N}\right]^{1/2}\right). \quad (7)$$

In Eqs. (6) and (7) n is the number concentration in the channel, N the integrated number concentration and D_p the particle diameter, i.e., the midpoint of the channel.

2.3 Calibrations

The measurements of volume mixing ratios taken inside the ship plumes are analyzed relative to the background, and therefore offset errors can be neglected. The accuracy over the dynamic range of interest was assured by frequent calibrations with standard gases, obtained from AGA and Air Liquide with mixing accuracies for CO_2 of 1 % and for SO_2 and NO_x around 5 %.

Usually the gases were measured from gas cylinders containing about 204 ppb NO_x, 401 and 407 ppb SO_2 as well as 370.5 and 410.6 ppm CO_2, respectively. During the last campaign, a standard Thermo 146i Dynamic Gas Calibrator was used instead together with a Thermo 1160 Zero Air Supply, mixing highly concentrated SO_2 and NO_x, both at 60 ppm, with filtered zero air. Mixing ratios of 400 ppb for SO_2 and 300 ppb for NO_x were used for calibration with the dynamic gas calibrator. The results were used to calculate a time series of respective calibration factors and offsets which in turn were used to post calibrate the plume measurements.

The calibrations were usually carried out on the ground before and after the measurement flights. The average precision of the measurements of the calibration gases was found

to be negligibly small for CO_2, 1.6 % for SO_2 and 0.5 % for NO_x.

The calibration factors that were applied to the measured values are linearly interpolated values from the nearest calibrations. The estimated interpolation error is the average of the standard deviations between adjacent calibration factors. This yields 0.1 % for CO_2, 5.4 % for SO_2 and 6.3 % for NO_x.

2.4 Uncertainties

The plumes of 158 different ships have been analyzed. Some ships were repeatedly measured on different occasions: in total 174 plumes were analyzed. The plumes were usually traversed several times for each occasion to improve the statistical validity of the measurements. An average of the precision for all measurements was calculated as the median value of the individual 1σ uncertainties of the respective emission factors for plumes that were traversed at least three times. For the calculated emission factors of SO_2 and NO_x in grams per kilogram fuel this yields measurement precisions of 19 and 22 %, respectively.

The overall uncertainties of the emission factors are calculated as the square root of the sum of all squared uncertainties due to calibrations and measurements for the respective gas species and CO_2. Hence, adding the square root of the quadratic sums for the SO_2 emission factor, this yields a total uncertainty of 20 % and correspondingly 24 % for the NO_x emission factor in grams per kilogram fuel. These uncertainties are comparable to the uncertainties of land-based measurements by Alföldy et al. (2013), who found values of 23 and 26 % for the emission factors of SO_2 and NO_x, respectively. It should be noted that the uncertainties of the measurements compare well, despite the fact that the plumes are sampled for much shorter periods when measured from aircrafts.

Earlier studies show that not all of the sulfur in the fuel is emitted as SO_2. Other experiments showed that 1 to 19 % of the sulfur in the fuel is emitted in other forms, possibly SO_3 or SO_4 (Schlager et al., 2006; Agrawal et al., 2008; Moldanova et al., 2009; Balzani Lööv et al., 2013; Moldanová et al., 2013). Hence the assumption that all sulfur is emitted as SO_2 yields an underestimation of the true sulfur content in the fuel.

An additional uncertainty for NO_x with regard to the IMO regulation is the fact that the emission factors are usually reported in grams per kilogram fuel, which requires a multiplication with the SFOC. Here, the uncertainty was estimated to be 11 %, assuming the real operation deviates from the test bed measurements of the SFOC. This estimation is based on the average deviation over the range of the SFOC values in the used model database. Thus the total uncertainty for the NO_x emission factor in grams per kilowatt-hour becomes 26.2 %.

A quantification of the uncertainties for the particle measurements has not been performed at this stage.

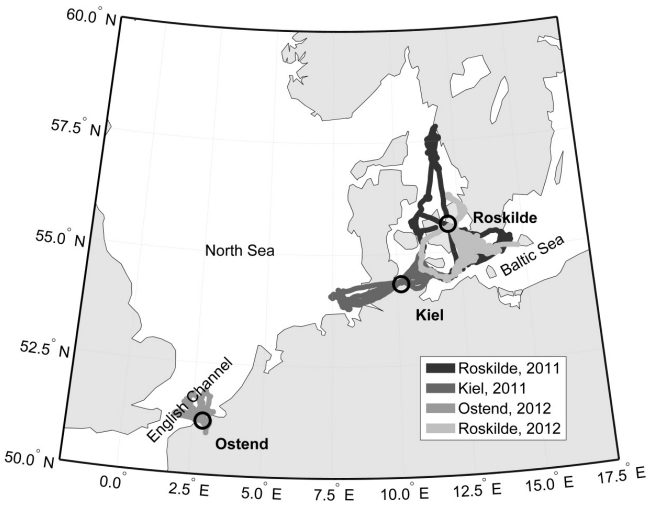

Figure 2. Map showing the flight tracks over the monitored sea regions for the different measurement campaigns; Roskilde (10–23 June 2011), Kiel (28 September–2 October 2011), Ostend (30 May–1 June 2012) and Roskilde (28 August–6 September 2012).

This EEPS instrument was tested by the manufacturer to ensure its conformity versus a scanning mobility particle sizer (SMPS) and a condensation particle counter (CPC) for 100 nm classified emery oil and polydisperse emery oil aerosols. It was found that the uncertainty in the measured sizes indicated a deviation of less than 7 %. A comparison with a CPC (TSI CPC 3022, $D_{p,min} = 7$ nm) indicated an uncertainty of better than 20 % for the total number of particles.

A quantification of the uncertainties for the particle measurements was performed in the local lab at Chalmers University of Technology alongside a SMPS consisting of TSI DMA 3081 and TSI CPC 3787. Ammonium sulfate was measured at different concentrations between 1.85 and 8.36×10^{11} particles m^{-3}. The standard deviation of the EEPS measurements was below 2 %. The comparison of the GMD between these instruments indicated that the results for the GMD measured with the EEPS are around 14 % below those measured with the SMPS in a particle size region around 30 nm.

2.5 Measurement campaigns

The results of four airborne measurement campaigns which were conducted in the years 2011 and 2012 are discussed in this paper. The flights were conducted from airports in Roskilde (Denmark), Kiel (Germany) and Ostend (Belgium). A summary of the presented measurement campaigns is given in Table 1. The measurements were made on 25 days within these periods. The campaigns covered different European sea areas, amongst those the English Channel and the German Bight, but in particular the western Baltic Sea. A map of the monitored regions is shown in Fig. 2.

Table 1. Description of the airborne measurement campaigns. Measurement flights were conducted on 25 days within these periods.

Period	Airport location	Monitored sea area	Aircraft	Measured substances
10–23 Jun 2011	Roskilde (DK)	Western Baltic Sea	Piper PA31	CO_2, SO_2
28 Sep–2 Oct 2011	Kiel (D)	Western Baltic Sea, German Bight	Partenavia P68B	CO_2, SO_2, NO_x, PN, PM
30 May–1 Jun 2012	Ostend (B)	English Channel	Eurocopter AS365 Dauphin	CO_2, SO_2, NO_x, PN, PM
28 Aug–6 Sep 2012	Roskilde (DK)	Western Baltic Sea	Piper PA31	CO_2, SO_2, NO_x

Figure 3. Instruments, mounted in racks, for ready installation in the Partenavia P68B airplane behind. The particle inlet can be seen on top of the fuselage (picture taken by B. Schneider, enviscope GmbH).

The measurements were conducted from airplanes, Piper PA31 and Partenavia P68B, and a helicopter of type Eurocopter AS365 Dauphin. The choice of instrumentation depended on the loading possibilities of the respective airborne vehicle. Inlet probes for gas measurements were sited beneath (Piper PA31) or on the side of the fuselage (Partenavia P68B and Dauphin helicopter) of the aircraft. The Partenavia was already equipped with an isokinetic inlet which was used for particulate matter measurements. The particle inlet on the Dauphin was mounted beside the gas inlet, at some distance from the fuselage to minimize effects due to the downwash of the main rotor. The minimum instrumental setup used during all campaigns consisted of a flight-modified Picarro G2301-m and a Thermo 43i-TLE for CO_2 and SO_2 measurements, respectively. NO_x was measured with the Thermo 42i-TL during all except the first campaign. The particle size distributions were measured with the EEPS onboard the Partenavia airplane and the Dauphin helicopter. A brief overview of the instrumental setup on each campaign is presented in Table 2. The Partenavia is shown together with the rack-mounted instrumental setup in Fig. 3.

2.6 Flight procedure during measurements

The aim of the IGPS project is to relate the measured emission plumes to individual ships. Therefore it is necessary to identify and locate the ships in the area surrounding the measurement. Ships from a certain size and upward are obliged to frequently broadcast their status by the AIS, which was received and logged during the measurement flights. This signal contains the ship identification number and name, its position, course and speed and further information. Together with information about the position of the aircraft and meteorological information, the source of an emission plume can be identified and connected to the determined emission parameters.

The flights took place above open waters with dense ship traffic. The AIS data were used for the selection and localization of the ships to be observed. Additionally, the AIS data contain information about the course and speed of the ship. Together with meteorological information about current wind speeds and directions, the plume position with respect to the ship can be calculated according to Berg et al. (2012). The AIS data are presented on the operator's screen like the example in Fig. 4 so ships can be selected before plume measurement and plumes can literally be related to them on the fly.

The plume height is usually between 50 and 70 m. The aircraft traverses the plume at these heights in a zigzag-shaped manner. So the emission of several transects through the plume of a ship can be measured. The distance from the ship for these maneuvers is between 25 m and 10 km. Ideally, the procedure begins at a further distance from the ship and the ship is approached with each new transect.

3 Results

Here the overall results of the measured ships are presented and discussed. Results for individual measurements can be found as supplemental material to this article.

3.1 SO_2 emission factors

The distribution of the number of the observed ships over their SO_2 emission factor is shown in the histogram in Fig. 5. The maximum of the distribution is found at $20\,g\,kg_{fuel}^{-1}$. The first and the third quartile of the SO_2 emission factors in the histogram are $15.8\,g\,kg_{fuel}^{-1}$ and $21.9\,g\,kg_{fuel}^{-1}$. This is reasonable because the IMO limit for sulfur in the fuel of ships in the observed region is 1 %, which corresponds to $20\,g\,kg_{fuel}^{-1}$. Hence, this maximum was expected as measurements were

Table 2. Overview of instrumentation used on the different platforms.

Parameter	Platform	Instrument	Method	Rise/fall time	Sampling rate
Carbon dioxide (CO_2)	Piper PA31 Partenavia P68B Dauphin	Picarro G2301-m	Cavity ring-down spectroscopy	< 1 s	1 Hz/2 Hz
Sulfur dioxide (SO_2)	Piper PA31 Partenavia P68B Dauphin	Thermo 43i-TLE (modified)	Fluorescence	2 s	1 Hz
Nitrogen oxides (NO_x)	Partenavia P68B Dauphin	Thermo 42i-TL (modified)	Chemiluminescence	< 1 s	1 Hz
Particle size distribution	Partenavia P68B Dauphin	TSI 3090	Electrical mobility	0.5 s	10 Hz

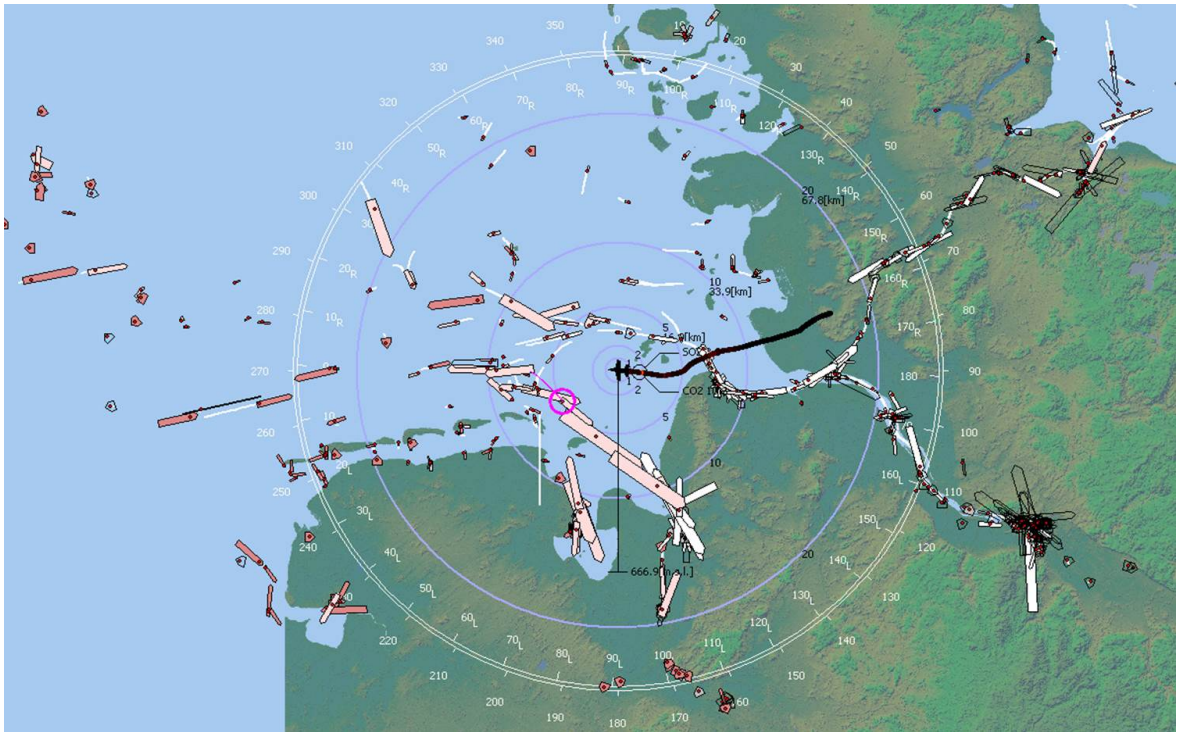

Figure 4. Map for real-time navigation purpose presented to the operator by IGPS software showing the current locations of surrounding ships and aircraft from the received Automatic Identification System (AIS) data sent by the ships. The different size of the ships corresponds to their gross tonnage. The blue circles around the aircraft's location indicate the distance to the ships and the time required to reach these. The two white circles provide information about ship locations relative to aircraft with respect to north and the current course of the aircraft.

taken mostly from commercially driven cargo, tanker and passenger vessels that were assumed for economic reasons to generally run close to the sulfur limit. Hence, a sharp decrease in the number of ships with SO_2 emission factors higher than 20 g kg_{fuel}^{-1} can be seen.

Yet, the SO_2 emission factors of four of the analyzed 174 ship plumes are between 40 and 44 g kg_{fuel}^{-1}. Two of these plumes originated from a fast Ro-Pax ferry which was observed on two different days during the campaign in Roskilde in 2011 – 15 June and 29 June with SO_2 emission factors 42.4 g kg_{fuel}^{-1} and 40.7 g kg_{fuel}^{-1}, respectively. The other two plumes with exceptionally high emission factors were emitted from a crude oil tanker and a cargo ship. Considering the uncertainty in the measurements of 20 % it can be found that around 15 % of all monitored ships do not comply with the sulfur limit of 1 %. This is not considering a systematic bias of 14 % for sulfur that is emitted in other forms than SO_2, as mentioned in the uncertainty analysis. The results of flight campaigns over the North and Baltic Sea conducted between 2007 and 2009 are shown in the inset in Fig. 5 (Mellqvist and Berg, 2010, 2014; Berg, 2011). A comparison of the median values of the SO_2 emission factor distributions indicates a reduction of 16 %. The assumed reason

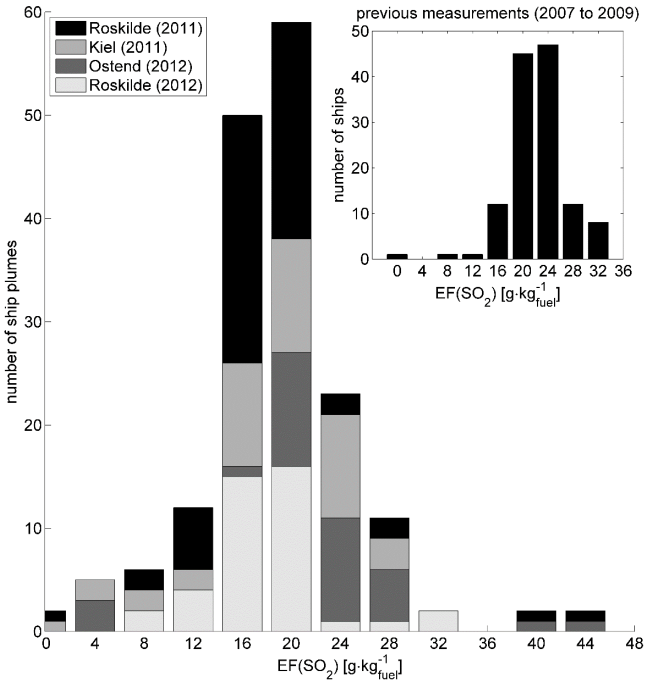

Figure 5. Histogram of the emission factor of SO_2, EF(SO_2), from airborne measurements for four campaigns (174 ships) in the years 2011 and 2012. The inset shows according results from earlier campaigns between 2007 and 2009 (127 ships). The comparison indicates a reduction of EF(SO_2). This coincides with the reduction of the limit of sulfer in fuel to 1 %. The corresponding values for the sulfur fuel content can be obtained by dividing the EF(SO_2) by 20.

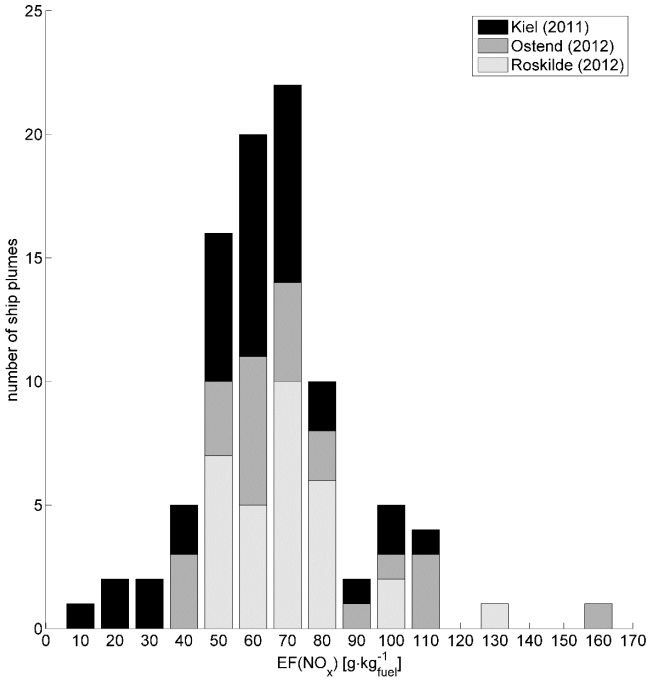

Figure 6. Histogram of the NO_x emission factor, EF(NO_x), relative to the amount of consumed fuel from airborne measurements for three campaigns in the years 2011 and 2012.

is that in 2010 the IMO changed the limit for the amount of sulfur in fuel in the North and Baltic Sea from 1.5 to 1 %.

3.2 NO_x emission factors

NO_x emissions were measured for 87 different vessels on 91 different occasions. The distribution of the number of analyzed ship plumes over NO_x emission factors is shown in Fig. 6. Most ships emit around 70 g kg_{fuel}^{-1} of NO_x. The first and third quartiles are 51.9 g kg_{fuel}^{-1} and 76.1 g kg_{fuel}^{-1}. The average NO_x emission factor related to the produced energy is 13.1 g kWh^{-1} with respective first and third quartiles of 10.4 g kWh^{-1} and 15.2 g kWh^{-1} for the measured plumes. In Table 3, the NO_x emission factors are presented for different crankshaft speeds. The highest emission factors with an average of 13.6 g kWh^{-1} were measured at slower engine speeds with a significant difference to emissions at engine speeds above 500 rpm. It should be noted that the IMO emission curves correspond to weighted emission averages of different loads, and this makes them difficult to compare with instantaneous emission. The engine types are tested under controlled lab conditions following specific driving cycles to determine the total weighted emission of NO_2 (MEPC, 2008). For a ship running close to its design speed, which is typically the case in this study, a difference between the emission factor at an arbitrary time and the IMO curve is foreseen for the ships. For instance, a typical slow-speed Wärtsilä engine has 15.8 g kWh^{-1} at 75 % load, while the NO_x weighted IMO value here is 3 % lower (T. Borkowski, personal communication, 9 June). For measurements of ships in harbors running at 25 % load this discrepancy becomes much larger. However, assuming that the instantaneous emissions at the time of the measurements that were evaluated for this study were representative, the Tier 1 limit would apply to 58 % and the Tier 2 limit to 7 % of the observed ships. Summarized, it was seen that 95 % of the analyzed ship plumes would comply with the respective NO_x limits assuming their instantaneous NO_x emission figures were representative, and taking into account the uncertainty of 24 %.

3.3 Particle emission factors

Size-resolved particle number distributions were measured between 15 and 560 nm at different distances to the vessel. Concentrations of particles with diameters under 15 nm were neglected due to high noise that occurred in the lower size channels of the EEPS. The distributions in the measured size range are monomodal.

The averaged particle diameters and emission factors at different distances to the emission source are presented in Table 4. The average geometrical mean diameter increases from 50 to 62 nm with increased distance. The full width

Table 3. NO_x emissions in relation to the rated engine speed of the ships. In total 91 plumes were analyzed. In this table, ships running on 2-stroke engines are found below 300 rpm. Ships with higher rated engine speeds were running with 4-stroke engines. In order to see if NO_x emissions are exceeding the IMO limits, the measurement uncertainty was considered. It should be considered that in contrast to IMO regulation the measurements only show the instantaneous emission and not the total weighted emission of NO_2 following the technical code on control of emissions of nitrogen oxides from marine diesel engines (MEPC, 2008).

Rated engine speed [rpm]	Average EF(NO_x) [$g\,kWh^{-1}$]	Average EF(NO_x) [$g\,kg_{fuel}^{-1}$]	Number of plumes	Number of plumes exceeding IMO limits
0...300	13.6 ± 5.3	71.3 ± 28.3	44	3
300...500	13.8 ± 2.4	67.9 ± 10.4	18	–
500...1000	12.0 ± 3.7	59.7 ± 18.3	28	2
1000...3000	5.2	26.1	1	–

Table 4. The geometric mean diameter (GMD), geometric standard deviation (GSD) and full width at half maximum (FWHM) as well as the emission factors for particle number and mass are shown. GMD, GSD and FWHM are related to the number size distributions. The values were averaged for intervals of the distance to ship at the moment the plume was traversed. Distances were retrieved for 202 transects.

Distance to ship [km]	GMD [nm]	GSD [nm]	FWHM [nm]	EF(PN) [$10^{16}\,kg_{fuel}^{-1}$]	EF(PM) [$mg\,kg_{fuel}^{-1}$]	Number of plume transects
0...0.5	44.8 ± 7.6	1.5 ± 0.1	42.8 ± 10.3	2.91 ± 1.59	2533 ± 1302	80
0.5...1	49.1 ± 15.7	1.4 ± 0.3	48.1 ± 15.9	2.41 ± 1.36	2947 ± 1762	32
1...2	51.4 ± 17.2	1.4 ± 0.4	49.5 ± 18.6	1.37 ± 1.05	3118 ± 5481	40
2...5	52.0 ± 18.8	1.3 ± 0.4	51.5 ± 22.2	0.99 ± 0.48	2078 ± 1673	31
5...8	53.4 ± 17.9	1.4 ± 0.4	52.1 ± 16.4	1.04 ± 0.67	2140 ± 1292	14

at half maximum of the distribution increases from 49 to 61 nm. In addition, the emission factor for particle number (PN) decreases with longer distance from 3 to 1×10^{16} particles kg_{fuel}^{-1}. The strongest gradient of the emission factor for the particle number as a function of distance to the ship can be seen for distances under 1 km. However, the emission factor for particle mass (PM) does not change significantly over distance from its average of 2770 $mg\,kg_{fuel}^{-1}$.

4 Discussion

The emission factors, sorted according to different ship types, are presented in Table 5. A comparison of the found results with other studies is given in Table 6.

The majority of the measured emissions originated from passenger ships, cargo ships and tankers. The SO_2 emission factors of these three types are around 19 $g\,kg_{fuel}^{-1}$. Trailing suction hopper dredger vessels show a much lower average SO_2 emission factor of 7.4 $g\,kg_{fuel}^{-1}$. Further, the presented emissions were measured from four different ships of this type. This picture was also reported for measurements taken at the harbor of Rotterdam in 2009 (Alföldy et al., 2013).

The NO_x emission factors are similar for the different ship types. The average was calculated to be 66.6 $g\,kg_{fuel}^{-1}$. However, it can be seen that cargo ships emit a slightly higher amount of NO_x compared to passenger ships and tankers. This is also described by Williams et al. (2009) for measurements in the Gulf of Mexico, showing that container carriers and passenger ships emit an average of 60 $g\,kg_{fuel}^{-1}$ while larger ships such as bulk freight carriers and tanker ships have average NO_x emissions of 87 and 79 $g\,kg_{fuel}^{-1}$, respectively. The averaged NO_x emission factors shown in Table 6 are in agreement with ship-borne measurements carried out by Williams et al. (2009) and Murphy et al. (2009), who describe simultaneous airborne and onboard measurements for one ship. Alföldy et al. (2013) made measurements on the shore side in the ship channel of Rotterdam, measuring an average NO_x emission factor of 53.7 $g\,kg_{fuel}^{-1}$, which they claim is in agreement with the EDGARv4.2 database (European Commission, 2009). This is significantly below the values found for the presented flight measurements, but can be explained with typically different engine load conditions in harbors.

The overall average of the PN emission factor is $1.8 \pm 1.3 \times 10^{16}$ particles kg_{fuel}^{-1} and for PM it is 2770 ± 1626 $mg\,kg_{fuel}^{-1}$. As presented in the comparison in Table 6, these values match very well with the spans of 0.3 to 6.2×10^{16} particles kg_{fuel}^{-1} and 0.4 to 5.3 $mg\,kg_{fuel}^{-1}$ found in other studies on ship emissions (Sinha et al., 2003; Chen et al., 2005; Petzold et al., 2008; Moldanova et al., 2009; Murphy et al., 2009; Petzold et al., 2010; Jonsson et al., 2011; Lack et al., 2011; Alföldy et al., 2013; Pirjola et al., 2014). In correlation with the decrease of the particle number emission factors, the GMD increases over distance, yet the particle masses are not changing significantly.

Table 5. Emission factors of SO_2, NO_x and particulate matter emissions for different ship types. The presented numbers are the mean values and standard deviations for each ship type of the average for each plume over several transects. The number in brackets is the number of plumes that have been traversed. The same ships may appear twice if they were measured on several occasions.

Ship type	EF(SO_2) [g kg_{fuel}^{-1}]	EF(NO_x) [g kg_{fuel}^{-1}]	EF(NO_x) [g kWh^{-1}]	EF(PM) [mg kg_{fuel}^{-1}]	EF(PN) [10^{16} kg_{fuel}^{-1}]
Passenger	19.1 ± 7.2 (34)	62.0 ± 19.3 (17)	11.9 ± 3.7 (17)	1680 ± 438 (5)	0.91 ± 0.18 (5)
Cargo	18.9 ± 6.2 (80)	70.3 ± 25.4 (45)	13.9 ± 4.8 (45)	3066 ± 1665 (37)	1.90 ± 1.31 (37)
Tanker	19.2 ± 5.8 (54)	65.4 ± 22.7 (24)	12.5 ± 4.2 (24)	2271 ± 875 (16)	2.01 ± 1.41 (16)
Trailing suction hopper dredger	7.4 ± 8.0 (4)	65.7 ± 5.6 (3)	14.3 ± 1.7 (3)	1725 ± 870 (3)	1.43 ± 0.21 (3)
Unspecified	23.2 ± 3.6 (2)	36.2 ± 14.2 (2)	8.0 ± 3.9 (2)	8362 (1)	1.79 (1)
All types	18.8 ± 6.5 (174)	66.6 ± 23.4 (91)	13.1 ± 4.4 (91)	2770 ± 1626 (62)	1.82 ± 1.26 (62)

Table 6. Comparison of the emission factors found in this study with the literature.

Reference (platform)	EF(SO_2) g kg_{fuel}^{-1}	EF(NO_x) g kg_{fuel}^{-1}	EF(NO_x) g kWh^{-1}	EF(PM) g kg_{fuel}^{-1}	EF(PN) 10^{16} kg_{fuel}^{-1}	Number of ships	Location (Year)
This study (airborne)	18.8 ± 6.5	66.6 ± 23.4	13.1 ± 4.4	2.8 ± 1.6	1.8 ± 1.3	174	Open sea, (2011/2012)
Sinha (2003)	2.9 ± 0.2[a]	22.3 ± 1.1[a]			4.0 ± 0.4[a]	2	Open sea (2000)
(airborne)	52.2 ± 3.7[b]	65.5 ± 3.3[b]			6.2 ± 0.6[b]		
Chen et al. (2005)	30 ± 4	20 ± 8			4.6 ± 1.4	2	Open sea (2002)
(airborne)	23 ± 7	13 ± 8			4.5 ± 1.8		
Petzold et al. (2008)					1.36 ± 0.24	1	Open sea (2004)
(airborne/onboard)							
Moldanova et al. (2009)	39.3	73.4	14.2	5.3		1	Open sea (2007)
(onboard)							
Murphy et al. (2009)	59.7 ± 0.5[c]	65.7 ± 0.3	20.1 ± 0.1		1.3 ± 0.2	1	Open Sea (2007)
(airborne/onboard)							
Williams et al. (2009)[d]	13.2 ± 10.4	66.4 ± 9.1				> 200	Open sea (2006)
(ship-borne)							
Petzold et al. (2010)					3.4 ± 1.3	1	Test rig, 85-100 % load
(test bed, stack)							
Jonsson et al. (2011)				2.05 ± 0.11	2.55 ± 0.11	734	Harbor (2010)
(land-based)							
Lack et al. (2011)	49 ± 7.5[e]			3.77 ± 1.3[e]	1.0 ± 0.2[e]	1	Open sea (2004)
(airborne)	4.3 ± 0.6[f]			0.39 ± 0.14[f]	1.4 ± 0.2[f]		
Alföldy et al. (2013)	6[a]	53.7			0.8[a]	497	Harbor (2009)
(land-based)	14...18[b]				1.8[b]		
Pirjola et al. (2014)	2.5...17	25...100		1.0...4.9[g]	0.32...2.26	11	Harbor & ship channel (2010/2011)
(land-based)							

[a] distillate fuel, [b] residual oil, [c] calculated from known SFC, [d] averaged data, only moving ships, [e] before fuel switch to low-sulfur fuel, [f] after fuel switch to low-sulfur fuel, [g] for $PM_{2.5}$.

Hence, coagulation is assumed to be the dominant factor. Considering that typical measured particle concentrations close to the ships are on the order of 1×10^{11} particles m^{-3} coagulation would be a significant process (Hinds, 1999; Willeke and Baron, 1993).

The PN and PM emission factors of the observed passenger ships are at the lower limit, whereas cargo ships and tankers show significantly higher emissions. Although only five plumes of four different passenger ships were analyzed for particulate matter emission factors, it appears that passenger ships emit about half as many particles as other ship types. The plumes of the passenger ships were traversed up to several kilometers away from the ship and the precision is comparatively high. Hence, this indicates that the PN emission factor of passenger ships generally is small compared to other types.

5 Summary and conclusions

Airborne in situ measurements of 174 ship plumes from 158 different ships at open sea were analyzed for this study. The emission factors of SO_2, NO_x and particles with particle diameters between 15 and 560 nm are presented.

The average SO_2 emission factor is 18.8 ± 6.5 g kg_{fuel}^{-1}. This corresponds to a sulfur fuel content of around 1 %, which was found for most of the studied ship plumes. The results show that approximately 85 % of the monitored ships comply with the limits defined by the IMO for sulfur content

in the observed sea regions. By comparison with earlier studies (Mellqvist and Berg, 2010, 2014; Berg, 2011), a reduction of the SO_2 emission factors after the reduction of the sulfur limit in 2010 was observed.

The average of the engine-dependent emission of NO_x is $66.6 \pm 23.4\,g\,kg_{fuel}^{-1}$. This compares very well to earlier studies conducted from measurement platforms on land, water and in the air.

The particle emission factors were presented relative to consumed fuel and engine power. The PN emission factors decrease with the distance to the plume, while the particle diameters increase, which was assumed to be due to coagulation. A strong gradient was found for distances up to 1 km.

The uncertainty for SO_2 and NO_x emissions in grams per kilogram fuel is, respectively, 20 % and 24 % and is comparable to the results of a land-based study (Alföldy et al., 2013). With this level of uncertainty, the developed system can be used for the identification of gross polluting ships from airborne platforms using the developed system. By using aircraft as operation platforms, the limitation of monitoring ships from stationary land-based sites becomes obsolete. Further, numerous ships can be reached and inspected within a short time, especially when they are making way at open sea. Another benefit of a moving over a stationary platform is that a changing wind direction is less critical, as the flight path can be adapted to the direction of the plume. The main drawback besides the costs in using airplanes is the very short time in which a plume is traversed at each transect, because better averaging could be achieved with longer sampling times for the plumes. On the other hand, samples can be taken repeatedly with aircraft. It is noteworthy that with measurements from aircraft, particles of the same plume can be sampled at different distances.

The system is presently installed more permanently in the mentioned Navajo Piper aircraft for compliance monitoring. In coming flight measurements additionally two optical devices will be used.

The Supplement related to this article is available online at doi:10.5194/amt-7-1957-2014-supplement.

Acknowledgements. The Swedish innovation agency Vinnova and the Swedish Environmental Protection Agency are acknowledged for financial support for the development of the IGPS measurement system and for carrying out the flight campaign through projects IGPS-2005-01835 and IGPS-plius-2008-03884. The Belgian DG environment (Directorate-General for the Environment of the Federal Public Service Health, Food Chain Safety and Environment) is thanked for providing support for the helicopter flights. We also acknowledge the assistance obtained from the helicopter provider NHV. We thank Gisela Carvajal for wind data and Tadeusz Borkowski for providing typical ship engine data.

Edited by: J. Hjorth

References

Agrawal, H., Malloy, Q. G. J., Welch, W. A., Wayne Miller, J., and Cocker, D. R.: In-use gaseous and particulate matter emissions from a modern ocean going container vessel, Atmos. Environ., 42, 5504–5510, doi:10.1016/j.atmosenv.2008.02.053, 2008.

Alföldy, B., Lööv, J. B., Lagler, F., Mellqvist, J., Berg, N., Beecken, J., Weststrate, H., Duyzer, J., Bencs, L., Horemans, B., Cavalli, F., Putaud, J.-P., Janssens-Maenhout, G., Csordás, A. P., Van Grieken, R., Borowiak, A., and Hjorth, J.: Measurements of air pollution emission factors for marine transportation in SECA, Atmos. Meas. Tech., 6, 1777–1791, doi:10.5194/amt-6-1777-2013, 2013.

Balzani Lööv, J. M., Alfoldy, B., Beecken, J., Berg, N., Berkhout, A. J. C., Duyzer, J., Gast, L. F. L., Hjorth, J., Jalkanen, J.-P., Lagler, F., Mellqvist, J., Prata, F., van der Hoff, G. R., Westrate, H., Swart, D. P. J., and Borowiak, A.: Field test of available methods to measure remotely SO_2 and NO_x emissions from ships, Atmos. Meas. Tech. Discuss., 6, 9735–9782, doi:10.5194/amtd-6-9735-2013, 2013.

Barone, T. L., Lall, A. A., Storey, J. M. E., Mulholland, G. W., Prikhodko, V. Y., Frankland, J. H., Parks, J. E., and Zachariah, M. R.: Size-resolved density measurements of particle emissions from an advanced combustion diesel engine: Effect of aggregate morphology, Energy Fuels, 25, 1978–1988, 2011.

Berg, N.: Remote measurements of ship emissions, Dept of Earth and Space Sciences, Chalmers University of Technology, Göteborg, Sweden, 2011.

Berg, N., Mellqvist, J., Jalkanen, J.-P., and Balzani, J.: Ship emissions of SO_2 and NO_2: DOAS measurements from airborne platforms, Atmos. Meas. Tech., 5, 1085–1098, doi:10.5194/amt-5-1085-2012, 2012.

Chen, G., Huey, L. G., Trainer, M., Nicks, D., Corbett, J., Ryerson, T., Parrish, D., Neuman, J. A., Nowak, J., Tanner, D., Holloway, J., Brock, C., Crawford, J., Olson, J. R., Sullivan, A., Weber, R., Schauffler, S., Donnelly, S., Atlas, E., Roberts, J., Flocke, F., Hubler, G., and Fehsenfeld, F.: An investigation of the chemistry of ship emission plumes during ITCT 2002, J. Geophys. Res.-Atmos., 110, D10S90, doi:10.1029/2004jd005236, 2005.

Cooper, D. A.: Exhaust emissions from ships at berth, Atmos. Environ., 37, 3817–3830, doi:10.1016/S1352-2310(03)00446-1, 2003.

Corbett, J. J., Winebrake, J. J., Green, E. H., Kasibhatla, P., Eyring, V., and Lauer, A.: Mortality from ship emissions: A global assessment, Environ. Sci. Technol., 41, 8512–8518, 2007.

European Commission: Joint Research Centre (JRC)/Netherlands Environmental Assessment Agency (PBL), Emission Database for Global Atmospheric Research (EDGAR), release version 4.0, available at: http://edgar.jrc.ec.europa.eu (last access: 26 June 2014), 2009.

Hallquist, Å. M., Fridell, E., Westerlund, J., and Hallquist, M.: Onboard measurements of nanoparticles from a SCR-equipped marine diesel engine, Environ. Sci. Technol., 47, 773–780, 2013.

Hinds, W. C.: Aerosol technology : properties, behavior, and measurement of airborne particles, Wiley, New York, 1999.

Hobbs, P. V., Garrett, T. J., Ferek, R. J., Strader, S. R., Hegg, D. A., Frick, G. M., Hoppel, W. A., Gasparovic, R. F., Russell, L. M., Johnson, D. W., O'Dowd, C., Durkee, P. A., Nielsen, K. E., and Innis, G.: Emissions from ships with respect to their effects on clouds, J. Atmos. Sci., 57, 2570–2590, 2000.

IHS Fairplay World Shipping Encyclopedia: available at: http://www.ihs.com/products/maritime-information/ships/world-shipping-encyclopedia.aspx (last access: March 2013), 2009.

Jalkanen, J.-P., Brink, A., Kalli, J., Pettersson, H., Kukkonen, J., and Stipa, T.: A modelling system for the exhaust emissions of marine traffic and its application in the Baltic Sea area, Atmos. Chem. Phys., 9, 9209–9223, doi:10.5194/acp-9-9209-2009, 2009.

Jalkanen, J.-P., Johansson, L., Kukkonen, J., Brink, A., Kalli, J., and Stipa, T.: Extension of an assessment model of ship traffic exhaust emissions for particulate matter and carbon monoxide, Atmos. Chem. Phys., 12, 2641–2659, doi:10.5194/acp-12-2641-2012, 2012.

Johnson, T., Caldow, R., Pöcher, A., Mirme, A., and Kittelson, D.: A new electrical mobility particle sizer spectrometer for engine exhaust particle measurements, SAE Technical Papers, 2004.

Jonsson, A. M., Westerlund, J., and Hallquist, M.: Size-resolved particle emission factors for individual ships, Geophys. Res. Lett., 38, L13809, doi:10.1029/2011GL047672, 2011.

Kalli, J., Karvonen, T., and Makkonen, T.: Sulphur content in ships bunker fuel in 2015 – A study on the impacts of the new IMO regulations and transportation costs, Ministry of Transport and Communications, Publications of the Ministry of Transport and Communications 31/2009, ISSN: 1795-4045, ISBN: 978-952-243-074-8, 2009.

Kley, D. and McFarland, M.: Chemiluminescence detector for NO and NO_2, Atmos. Technol., 12, 63–69, 1980.

Lack, D. A., Cappa, C. D., Langridge, J., Bahreini, R., Buffaloe, G., Brock, C., Cerully, K., Coffman, D., Hayden, K., Holloway, J., Lerner, B., Massoli, P., Li, S. M., McLaren, R., Middlebrook, A. M., Moore, R., Nenes, A., Nuaaman, I., Onasch, T. B., Peischl, J., Perring, A., Quinn, P. K., Ryerson, T., Schwartz, J. P., Spackman, R., Wofsy, S. C., Worsnop, D., Xiang, B., and Williams, E.: Impact of fuel quality regulation and speed reductions on shipping emissions: implications for climate and air quality, Environ. Sci. Technol., 45, 9052–9060, doi:10.1021/es2013424, 2011.

Luke, W. T.: Evaluation of a commercial pulsed fluorescence detector for the measurement of low-level SO_2 concentrations during the gas-phase sulfur intercomparison experiment, J. Geophys. Res. Atmos., 102, 16255–16265, 1997.

Mellqvist, J. and Berg, N.: Final Report to Vinnova: Identification of gross polluting ships, RG Report No. 4, ISSN 1653 333X, Chalmers University of Technology, Göteborg, 2010.

Mellqvist, J. and Berg, N.: Airborne surveillance of sulfur and NO_x in ships as a tool to enforce IMO legislation, Atmos. Meas. Tech. Discuss., in preparation, 2014.

Mellqvist, J., Berg, N., and Ohlsson, D.: Remote surveillance of the sulfur content and NO_x emissions of ships, Second international conference on Harbors, Air Quality and Climate Change (HAQCC), Rotterdam, The Netherlands, 29–30 May, 2008.

MEPC: Marine Environment Protection Commitee, Amendments to the technical code on control of emission of nitrogen oxides from marine diesel engines – NO_x Technical Code, 2008.

Moldanova, J., Fridell, E., Popovicheva, O., Demirdjian, B., Tishkova, V., Faccinetto, A., and Focsa, C.: Characterisation of particulate matter and gaseous emissions from a large ship diesel engine, Atmos. Environ., 43, 2632–2641, doi:10.1016/j.atmosenv.2009.02.008, 2009.

Moldanová, J., Fridell, E., Winnes, H., Holmin-Fridell, S., Boman, J., Jedynska, A., Tishkova, V., Demirdjian, B., Joulie, S., Bladt, H., Ivleva, N. P., and Niessner, R.: Physical and chemical characterisation of PM emissions from two ships operating in European Emission Control Areas, Atmos. Meas. Tech., 6, 3577–3596, doi:10.5194/amt-6-3577-2013, 2013.

Murphy, S., Agrawal, H., Sorooshian, A., Padró, L. T., Gates, H., Hersey, S., Welch, W. A., Jung, H., Miller, J. W., Cocker Iii, D. R., Nenes, A., Jonsson, H. H., Flagan, R. C., and Seinfeld, J. H.: Comprehensive simultaneous shipboard and airborne characterization of exhaust from a modern container ship at sea, Environ. Sci. Technol., 43, 4626–4640, 2009.

O'Keefe, A. and Deacon, D. A. G.: Cavity ring-down optical spectrometer for absorption measurements using pulsed laser sources, Rev. Sci. Instrum., 59, 2544–2551, 1988.

Petzold, A., Feldpausch, P., Fritzsche, L., Minikin, A., Lauer, P., and Bauer, H.: Particle emissions from ship engines, J. Aerosol. Sci., 35, S1095–S1096, 2004.

Petzold, A., Hasselbach, J., Lauer, P., Baumann, R., Franke, K., Gurk, C., Schlager, H., and Weingartner, E.: Experimental studies on particle emissions from cruising ship, their characteristic properties, transformation and atmospheric lifetime in the marine boundary layer, Atmos. Chem. Phys., 8, 2387–2403, doi:10.5194/acp-8-2387-2008, 2008.

Petzold, A., Weingartner, E., Hasselbach, J., Lauer, P., Kurok, C., and Fleischer, F.: Physical properties, chemical composition, and cloud forming potential of particulate emissions from a marine diesel engine at various load conditions, Environ. Sci. Technol., 44, 3800–3805, 2010.

Pirjola, L., Pajunoja, A., Walden, J., Jalkanen, J.-P., Rönkkö, T., Kousa, A., and Koskentalo, T.: Mobile measurements of ship emissions in two harbour areas in Finland, Atmos. Meas. Tech., 7, 149–161, doi:10.5194/amt-7-149-2014, 2014.

Schlager, H., Baumann, R., Lichtenstern, M., Petzold, A., Arnold, F., Speidel, M., Gurk, C., and Fischer, H.: Aircraft-based Trace Gas Measurements in a Primary European Ship Corridor, TAC-Conference, Oxford, UK, 2006,

Sinha, P., Hobbs, P. V., Yokelson, R. J., Christian, T. J., Kirchstetter, T. W., and Bruintjes, R.: Emissions of trace gases and particles from two ships in the southern Atlantic Ocean, Atmos. Environ., 37, 2139–2148, doi:10.1016/S1352-2310(03)00080-3, 2003.

Tuttle, K. L.: Combustion-generated emissions in marine propulsions systems, Proceedings of the SNAME 1994 Environmental Symposium – Ship Design and Operation in Harmony with the Environment, Society of Naval Architects and Marine Engineers, Jersey City, NJ, 1995, 311–323, 1995.

Virtanen, A., Ristimäki, J., Marjamäki, M., Vaaraslahti, K., Keskinen, J., and Lappi, M.: Effective density of diesel exhaust particles as a function of size, SAE Technical Papers, 2002.

Willeke, K. and Baron, P. A.: Aerosol measurement: principles, techniques, and applications, Van Nostrand Reinhold, New York, 1993.

Williams, E. J., Lerrier, B. M., Murphy, P. C., Herndon, S. C., and Zahniser, M. S.: Emissions of NO_x, SO_2, CO, and HCHO from commercial marine shipping during Texas Air Quality Study (TexAQS) 2006, J. Geophys. Res. Atmos., 114, D21306, doi:10.1029/2009JD012094, 2009.